The Egyptian Journal of Hospital Medicine (July 2023) Vol. 92, Page 5528-5539

Role of Magnetic Resonance Imaging in Evaluation of Non-Traumatic Spinal Lesions in Children

Hayam Abdelmonsif Abdellatif, Ahmed Yassen El-Refaey*, Hazem Hassan Eid
Radio Diagnosis, Faculty of Medicine, Menoufia University, Menoufia, Egypt
***Corresponding author:** Ahmed Yassen El-Refaey, **Mobile:** (+20) 01000853271, **Email:** a7medyassen99@gmail.com

ABSTRACT

Background: A wide range of disorders, including those with inflammatory, viral, neoplastic, vascular, metabolic, and traumatic origins, can affect the spinal cord. Spinal cord lesions may often be distinguished between neoplastic and non-neoplastic using MRI.

Objective: This study aimed to evaluate the relevance of MRI in the diagnosis of children non-traumatic spinal lesions.

Patient and Method: A cross-sectional analytic study was conducted on 50 of either child presented with non-traumatic spinal lesions to be evaluated at our Radiology Department, Faculty of Medicine, Menoufia University by Magnetic Resonance Imaging during a period time from January to December 2022. All patients included in the current study were diagnosed based on clinical examination, and other main imaging modalities.

Results: The most common MR diagnosis was myelomeningocele (18%) then meningitis (12%) followed by focal kyphus deformity, Guillain Barre syndrome, intramedullary abscess, and astrocytoma (10%), osteoblastoma, lipoma and diastematomyelia (8%) and Tethered cord (6%).

Conclusion: MRI is the best way in evaluation of non-traumatic spinal lesions in children.

Keywords: Magnetic resonance imaging, Metastatic lesions, Neoplasm, Spinal lesions**.**

INTRODUCTION

Paediatric populations seldom get spinal tumours. In contrast to adult spinal disorders, paediatric versions exhibit a variety of unique characteristics. For instance, up to 85% of individuals with chronic pain lasting more than two months in children have a particular diagnosable lesion. Clinical signs of spinal tumours may also include fever, weakness, weight loss, neurological impairments, bowel, and bladder dysfunction, and more [1].

Anatomic position with regard to the vertebral end plate (vertebral corner versus noncore) and presence in either central (containing the spinal canal) or lateral (excluding the spinal canal) sagittal slices are used to characterise inflammatory lesions, respectively [1]. Ankylosing spondylitis (AS) individuals who have spinal inflammation have significant morbidity, which might potentially result in disability due to the axial skeleton's gradual ossification. By anatomic location (facet joint, spinous process), inflammatory lesions are also noted in the posterior parts of the spine [2].

Occult spinal dysraphism is a category that includes lesions when the deformed neural tissue is located deep within an intact skin cover. Dorsal dermal sinus, spinal lipoma, tight filum terminale syndrome, neuroenteric cyst (NEC), and diastematomyelia are among the diverse collection of lesions that make up this condition. These lesions are characterised by a split in the spinal cord and/or a caudal mass, a bone spur, or a fibrous band tying the spinal cord in an unusually low position [3].

The ability to distinguish between neoplastic and non-neoplastic spinal cord lesions is often enabled by MRI, however its ability to define tumour histology is constrained. The complete spine should always be included in an MRI, and the brain should also be included if a localized spinal cord neoplasm is found in order to rule out secondary or metastatic lesions [4].

Metastatic lesions from an intracranial tumour may manifest as spinal lesions. Multiple planes should be used in MRI procedures to benefit from various imaging contrasts, such as T1- and T2-weighted images. Images with more contrast will have higher diagnostic sensitivity. Finally, functional sequences like 1H magnetic resonance spectroscopy (MRS) and diffusion tensor imaging (DTI) may be useful [5]. There are increasingly more MRI sequences available that are less susceptible to susceptibility artefacts. A tiny needle biopsy is advised after radiological assessment to confirm the tumor's histology and direct therapy, as well as laboratory evaluation to check for systemic illness [6]. This study aimed to evaluate the relevance of MRI in the diagnosis of children non-traumatic spinal lesions.

PATIENTS AND METHODS

A cross-sectional analytic study was conducted on 50 of either child presented with non-traumatic spinal lesions to be evaluated at our Radiology Department, Faculty of Medicine, Menoufia University by Magnetic Resonance Imaging during the period from January to December 2022. All patients included in the current study were diagnosed based on clinical examination, and other main imaging modalities.

Inclusion criteria: Patients with spinal lesion based on clinical and laboratory evaluation to detect MRI criteria and extent of lesion, both sexes, ages up to 18 years old, patients known to have tumor refereed for initial staging (TNM) staging and planning for treatment and underwent preoperative MR imaging and known spinal lesions for follow-up by MRI.

Exclusion criteria: Patients who have allergy to MRI contrast media, Contraindication of MRI e.g., metal, prosthesis and ages >18 years.

Received: 23/03/2022
Accepted: 24/05/2023

Methods:

All patients included in the study were subjected to the following: history taking including age, sex, age of onset, disease duration, residence, past and present history of any disease. Also, full details of clinical symptoms including pain, fever, weight loss, weakness, neurological deficits, bowel and bladder dysfunction, and more. MRI imaging was performed with 1.5 T MR system. The images were performed with different MRI sequences and indifferent planes. MR imaging features of spinal lesions and adjacent cord were characterized by type of lesion, number of lesions, site of lesion vertebral bone and intervertebral space change.

MRI protocol: Imaging were performed with 1.5T magnet. Spinal coils, which are integrated into the MRI table, were used in this investigation. It is unclear what the ideal spinal magnetic resonance imaging procedure should be. For imaging patients with sciatica and/or lumbar pain, sagittal T2 weighted FSE, sagittal T1 weighted SE, and axial T2 weighted FSE sequences are all extensively used. The selection of sequences is substantially more difficult in the investigation of the cervical spine because to the restricted volume of CSF compared to the lumbar spine. In regular cervical spine imaging, sagittal T2 FSE, sagittal T1 SE, and axial 2D GE pictures are recommended. On both lumbar and cervical spine exams, a STIR sequence can be included to this technique to evaluate the bone marrow. The picture quality produced by the 2D GE is sufficient to distinguish between the disc and bony protrusions. In the literature, there is still debate concerning using FLAIR to image spinal cord injuries.

Ethical consideration: The Medical Research Ethics Committee of the Faculty of Medicine, Menoufia University approved the study. Written informed permission was acquired from the parents before they participated in the study. The Helsinki Declaration, the World Medical Association's code of ethics for human studies, governed the conduct of this study.

Statistical analysis

The data was tabulated and statistically analysed using a standard computer tool, SPSS V.25. One type of statistics was conducted. The mean (±) SD was used to represent quantitative data, and frequency and percentage were used to express qualitative data. By averaging each observation by the total number of observations, the mean is computed. The standard deviation measures the degree of dispersion among individual variations around their mean. P value ≤ 0.05 was regarded as significant.

RESULTS

The mean age was 5.16 ± 4.94 years. Females (62%) were higher than males (38%). According to distribution of the studied patients regarding type, location, and number of lesions, the most common type was intramedullary (48%) then extradural (36%) and intradural extramedullary (16%). The most common location was lumbar and cauda equina, lumbosacral (18%) than another location. The most common number of lesions was multiple (66%) then solitary (34%) (Table 1).

Table (1): Demographic data and distribution of the studied patients regarding type, location, and number of lesions (n=50)

	Patients (n=50)	
	Mean ± SD	**Range**
Age	5.16 ± 4.94	0.33-15
Sex	**N**	**%**
Male	19	38
Female	31	62
Distribution of the studied patients		
Type		
-Extradural	18	36.0
-Intradural	8	16.0
extramedullary	24	48.0
-Intramedullary		
Location		
- Lumbar	6	12.0
- Dorso-	5	10.0
Lumbar-	9	18.0
Junction	5	10.0
- Lumbar and	9	18.0
cauda equina	6	12.0
- Dorso-Lumbar	5	10.0
- Lumbosacral		
- Cervical and		
cauda equina		
- Cauda equina		
Number of lesions		
- Multiple	33	66.0
- Solitary	17	34.0

Moreover, most of patients were living in rural areas (72%), 70% patients had past history, 70% had pain, 40% had fever, 34% had weight loss, 60% had weakness, 48% had neurological deficits and 14 % had bowel and bladder dysfunction. According to distribution of the studied patients regarding effects of lesion, paraspinal masses were 24 %, vertebral bone involvement was 42%, cord compression was 30% and cord expansion was 0%. Regarding MR diagnosis, the most common MR diagnosis was myelomeningocele (18%) then meningitis (12%) followed by focal Kyphus deformity, Guillain Barre Syndrome, intramedullary abscess and astrocytoma (10%), osteoblastoma, lipoma and diastematomyelia (8%) and tethered cord (6%) (Table 2).

Table (2): History, symptoms and distribution of the studied patients regarding effects of lesion and MR diagnosis among the studied groups

	Patients (n=50)	
	No	**%**
Residence -		
Urban	14	28
-Rural	36	72
Past history		
No	15	30.0
Yes	35	70.0
Pain		
Yes	35	70.0
No	15	30.0
Fever		
Yes	20	40
No	30	60
Weight loss		
Yes	17	34
No	33	66
Muscle Weakness		
Yes	30	60
No	20	40
Neurological deficits		
Yes	24	48
No	26	52
Bowel and bladder dysfunction		
Yes	7	14
No	43	86
Effects of lesion		
Paraspinal mass		
Yes	12	24.0
No	38	76.0
Vertebral bone involvement		
Yes	21	42.0
No	29	58.0
Cord compression		
Present	15	30.0
Absent	35	70.0
Cord expansion		
Yes	0	0.0
No	50	100.0
MR diagnosis		
Tethered cord	3	6.00
Osteoblastoma	4	8.00
Focal Kyphus deformity	5	10.00
Guillain Barre syndrome	5	10.00
Intramedullary abscess	5	10.00
Meningitis	6	12.00
Myelomeningocele	9	18.00
Lipoma	4	8.00
astrocytoma	5	10.00
Diastematomyelia	4	8.00

The current study reported that hyperintense T1WI were 46%. While hyperintense T2WI were 38%. According to distribution of the studied patients regarding post contrast enhancement, post contrast enhancement was 50%. According to distribution of the studied patients regarding associated findings, tethered cord association was (10%) (Table 3).

Table (3): MRI signal of intraspinal tumors in relation to the cord and distribution of the studied patients regarding post contrast enhancement and associated findings

MRI appearance of intraspinal tumors	**Patients(n=50)**	
	No	%
T1WI		
Normal	27	54.0
Hyperintense	23	46.0
T2 WI		
Normal	31	62.0
Hyperintense	19	38.0
Post contrast enhancement		
Yes	25	50
No	25	50
Association		
Tethered cord	5	10.0
No	45	90.0

Astrocytoma was found in 3 females in normal T1 and T2, osteoblastoma was found in 3 females in hyperintense T1 and T2. Focal Kyphosis deformity was found in 5 females in normal T1and T2. Guillain Barre Syndrome was found in 5 females in normal T1 and T2. Intramedullary abscess was found in 5 females in normal T1 and T2. Meningitis was found in 6 males in hyperintense T1 and T2. Meningocele was found in 4 males in hyperintense T1 and normal T2. Lipoma was found in 5 males in hyperintense T1 and T2 (Table 4).

Table (4): MRI of Extradural tumor regarding T1 and T2

Lesion	**Sex**	**MRI features**			
		T1		**T2**	
		Normal	**Hyperintense**	**Normal**	**Hyperintense**
Astro-cytoma	Female	3	--	3	--
Osteo-blastoma	Female	--	3	--	3
Focal Kyphus deformity	Female	5	--	5	--
Guillain Barre syndrome	Female	5	--	5	--
Intra-medullary abscess	Female	5	--	5	--
Meningitis	Male	--	6	--	6
Myelomeningocele	Male	--	4	4	--
Lipoma	Male	--	5	--	5

Regarding post-contrast enhancement in MRI features, astrocytoma was found in 3 female, Guillain

Barre Syndrome was found in 5 females. Meningitis was found in 6 males **(Table 5)**.

Table (5): MRI of Extradural tumor regarding post contrast enhancement

Lesion	Sex	MRI features	
		Post contrast enhancement	
		Yes	No
astrocytoma	Female	**3**	--
Osteoblastoma	Female	--	**3**
tethered cord	Female	--	**5**
Guillain Barre syndrome	Female	**5**	--
Intramedullary abscess	Female	--	**5**
Meningitis	Male	**6**	--
Myelomeningocele	Male	--	**4**
Lipoma	Male	--	**5**

Regarding vertebral bone involvement in MRI features, astrocytoma was found in 3 females, osteoblastoma was found in 3 females. Focal Kyphus deformity and intramedullary abscess were found in 5 females (Table 6).

Table (6): MRI of Extradural tumor regarding vertebral bone involvement.

Lesion	Sex	MRI features	
		Vertebral bone involvement	
		Yes	No
astrocytoma	Female	**3**	--
Osteoblastoma	Female	**3**	--
Focal Kyphus deformity	Female	**5**	--
Guillain Barre syndrome	Female	--	**5**
Intramedullary abscess	Female	**5**	--
Meningitis	Male	--	**6**
Myelomeningocele	Male	--	**4**
Lipoma	Male	--	**5**

ILLUSTRATIVE CASES

Case (1): Regarding cases study, in case 1, Male patient 4 years old presented by sacral swelling. Axial T1, axial T2, sagittal T1 and sagittal T2 revealed intradural extramedullary lesion (red arrows) at the level of S2 to S5 with tethered cord and another subcutaneous lesion at the same level, show hyperintense signal in T1WI and less hyperintense in T2WI with no contrast injection (black arrows). This patient was diagnosed as subcutaneous and cord lipoma.

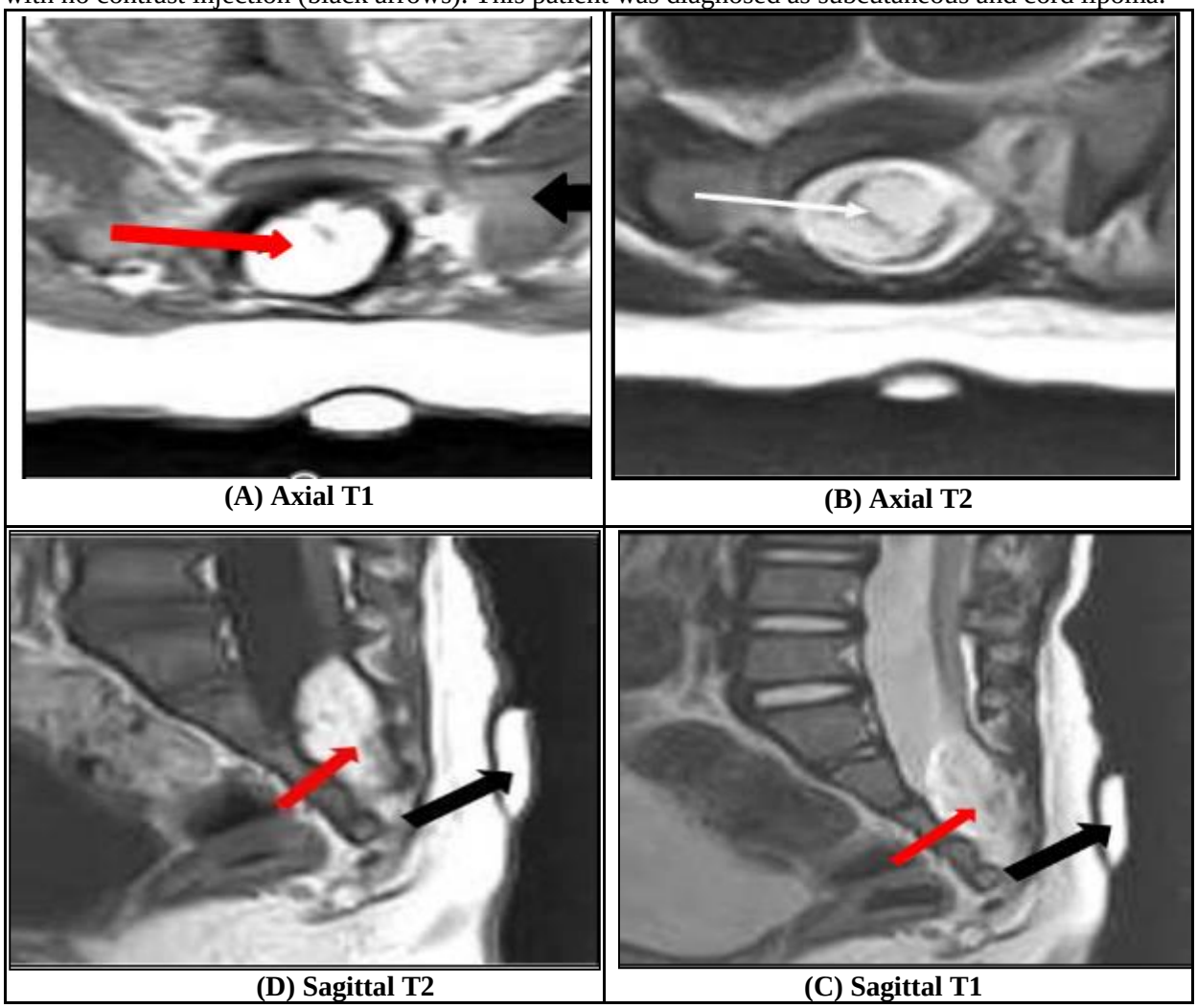

(A) Axial T1 **(B) Axial T2**

(D) Sagittal T2 **(C) Sagittal T1**

CASE (2)

13-years-old female patient with urinary incontinence, limb weakness, foot malposition, and low back discomfort were all symptoms. MRI results: Two hemicords may be seen in the lumbosacral spine on coronal, sagittal, and axial T2-weighted images, each of which is encircled by its own dural sac (arrowheads) and is divided from the other by an osteocartilaginous or bony spur (black arrows). The diastematomyelia is cranial to a hydrosyringomyelic cavity (dashed arrow). Diastematomyelia was identified as the patient's condition.

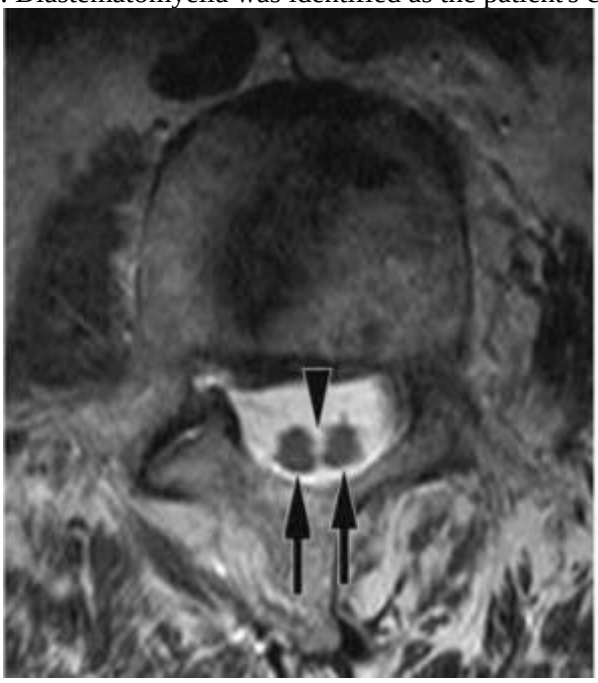

(A): Axial T2

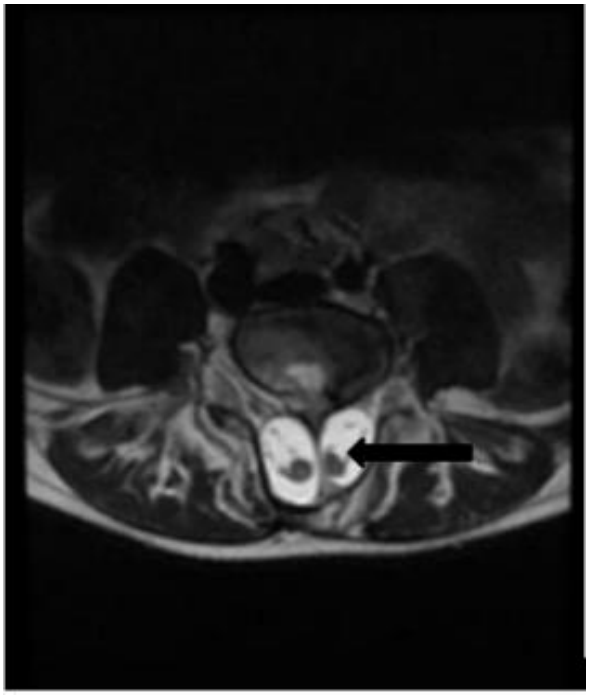

(B): Axial T2

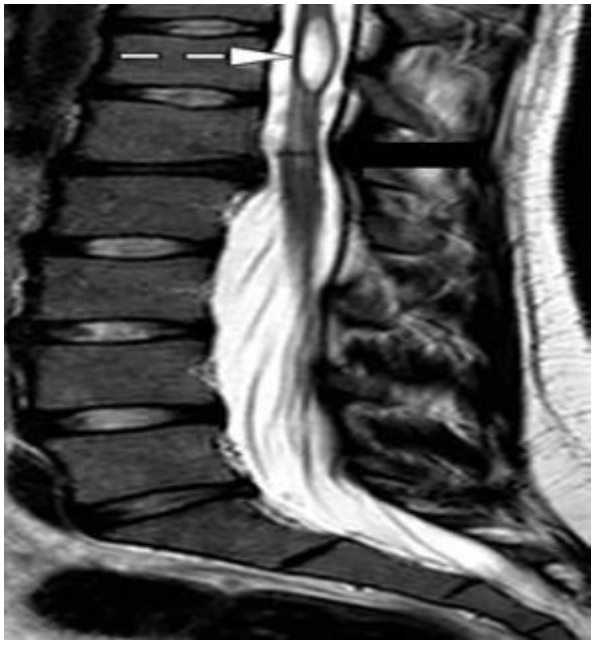

(C): Sagittal T2

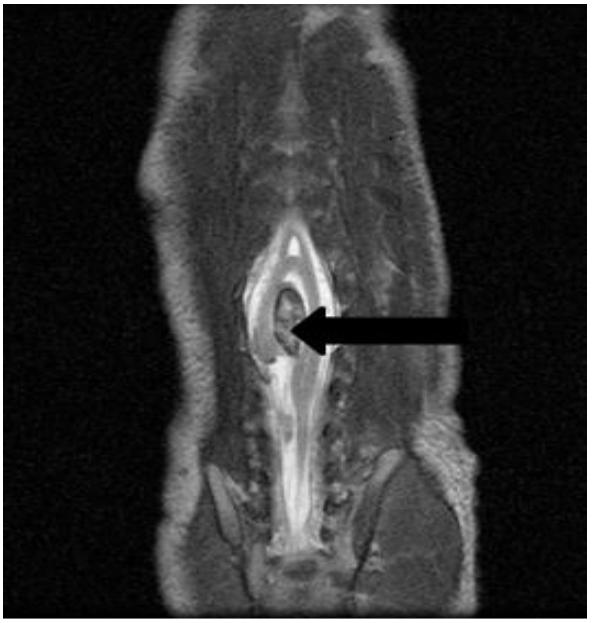

(D): Coronal T2

CASE (3)

Female patient 1.5 years old presented by slowly progressive weakness. MRI findings: Axial T1, T2 and T1 with contrast (A, B, C) and sagittal T2 and T1 with contrast (D, E). MRI showed intramedullary soft tissue lesion with significant cord expansion hypointense in T1. Contrast-enhanced T1-W MRI showed low enhancement (red arrows). This patient was diagnosed with astrocytoma.

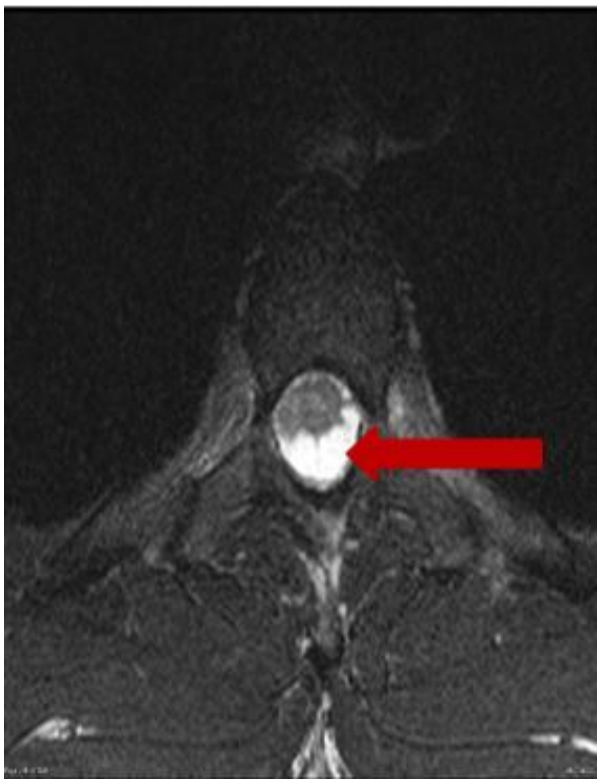

(A): Axial T2

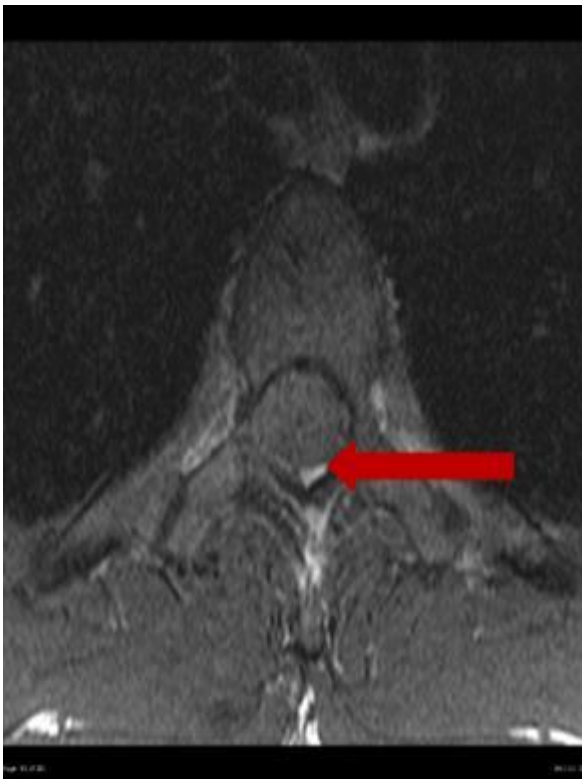

(B): Axial T1

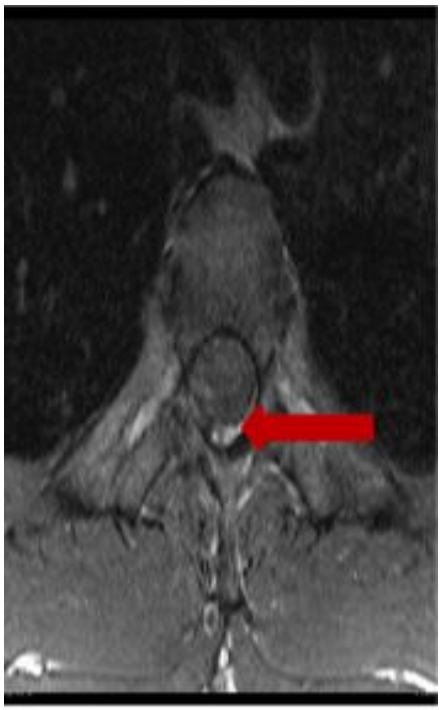

(C): Axial T1 C^+

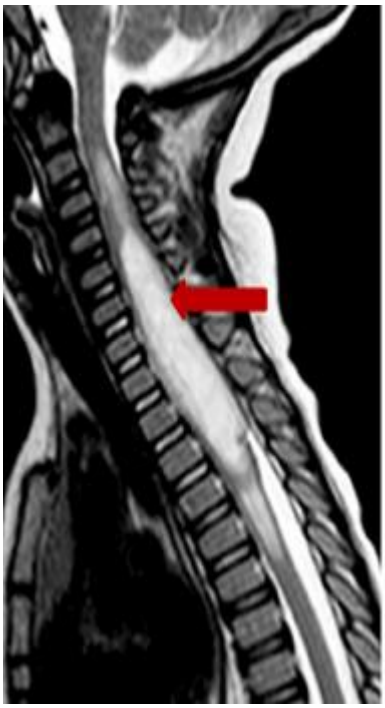

(D): Sagittal T2

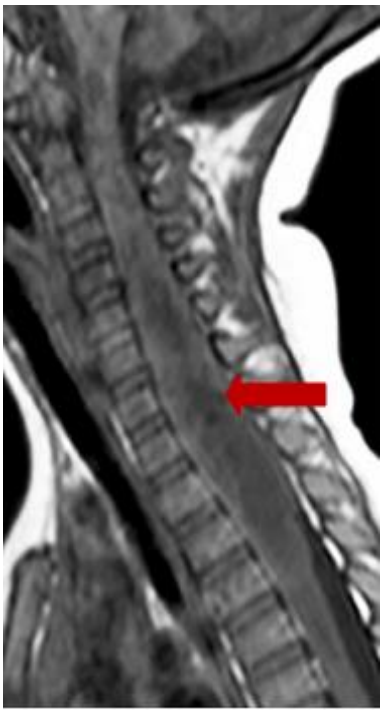

(E): Sagittal T1 C^+

CASE (4)

Female patient 1.5 years old presented by fever and vomiting. Sagittal T1 postcontrast and Sagittal T2 images (A and B) show 2 rims enhancing intradural abscesses. The more superior abscess is an intramedullary abscess in the conus medullaris. C and D, Axial T1 postcontrast and Axial T2 images (blue arrows) demonstrate intramedullary abscess within the conus, this patient was diagnosed with Intramedullary abscess.

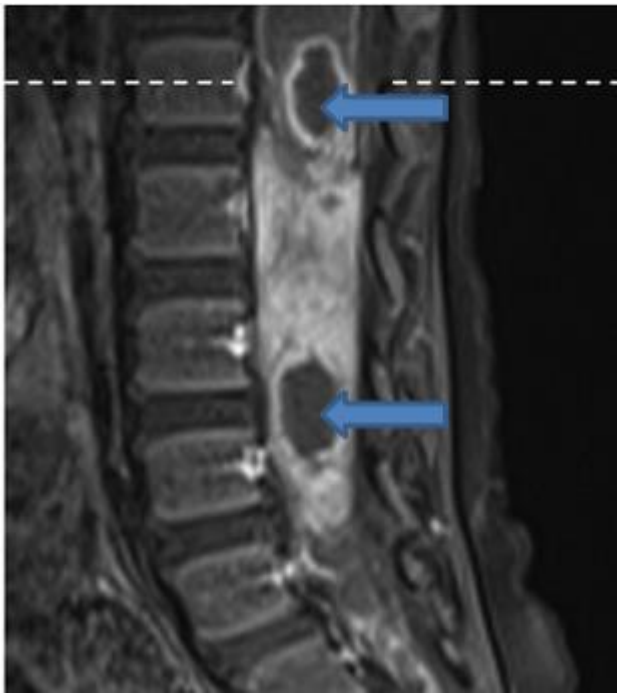

(A) Sagittal T1+C

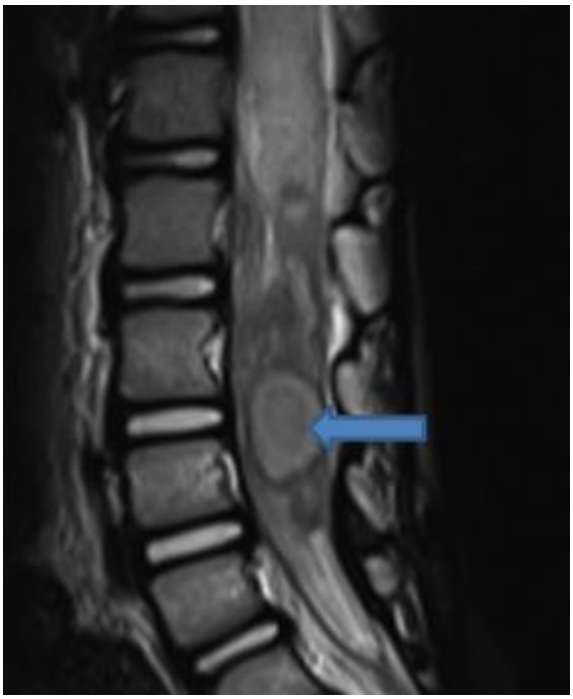

(B) Sagittal T2

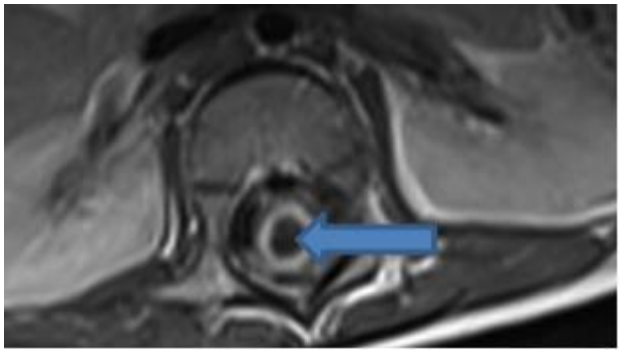

(C) Axial T1 +C

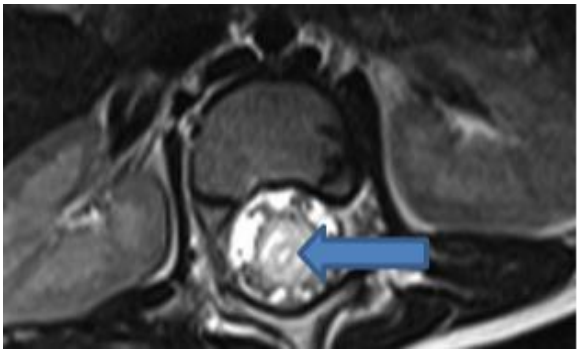

(D) Axial T2

CASE (5)

Male patient 6 months old presented by back swelling with bladder and bowel disfunction. Sagittal and axial oblique, single-shot fast spin-echo T2-weighted MR images of the fetal central nervous system show discontinuity of skin and subcutaneous tissue (arrowheads) in the lumbosacral region with herniation of nervous tissue through the spina bifida (thin arrows). This patient was diagnosed with Myelomeningocele.

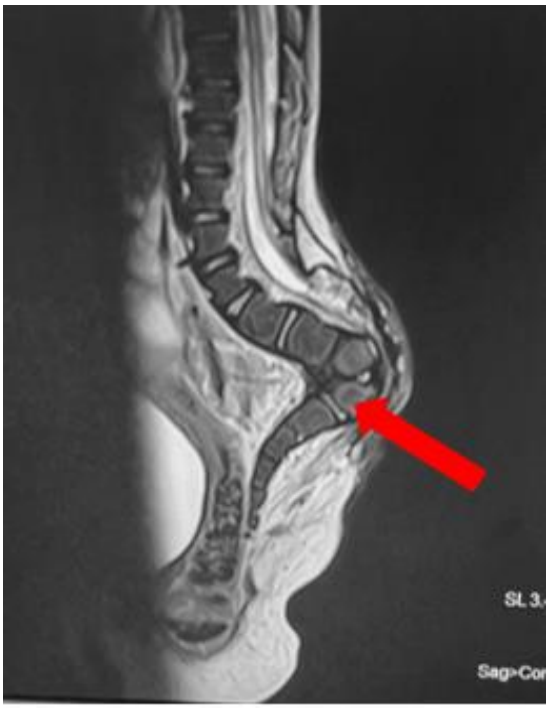

(A) Sagittal oblique, single-shot fast spin-echo T2

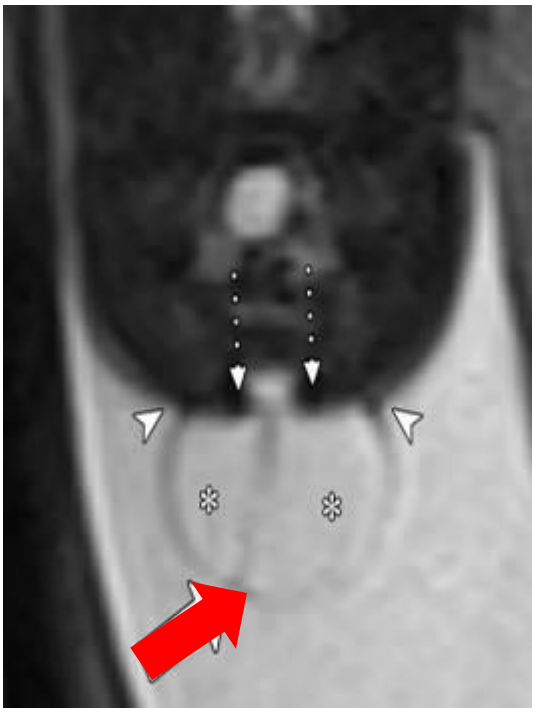

(B) axial oblique, single-shot fast spin-echo T2

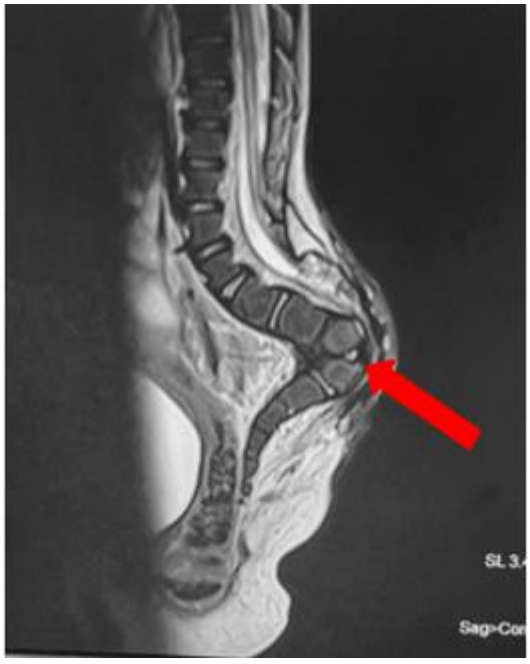

(C) Sagittal T2

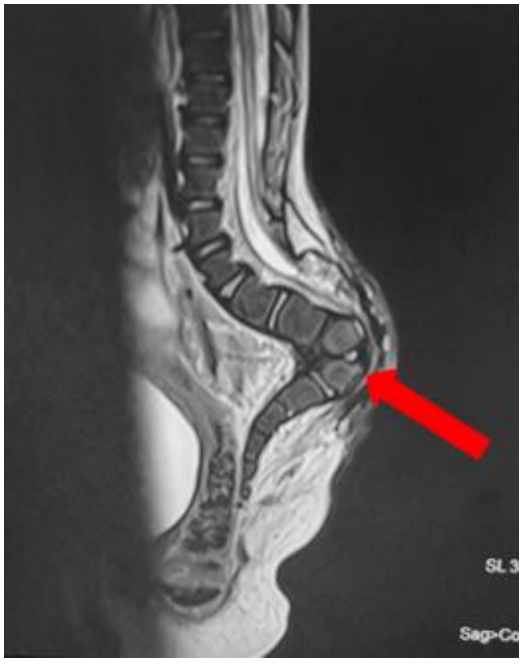

(D) Sagittal T2

CASE (6)

Female patient 2 years old presented by Muscle Weakness. Sagittal T1-weighted image (A) and fat-saturated image (B) The distal spinal cord is abnormally low (small arrow), terminating at the L4-5 level. The spinal cord terminates into a globular region of soft tissue lesion beginning at L5 (large arrow) that is of increased T1 signal intensity and is of homogeneous decreased signal intensity on the fat-saturated sequence and is compatible with a fat. Sagittal T1 weighted image (c) and axial T2 (D) show that the distal spinal cord is abnormally low (yellow arrows). This patient was diagnosed with tethered cord.

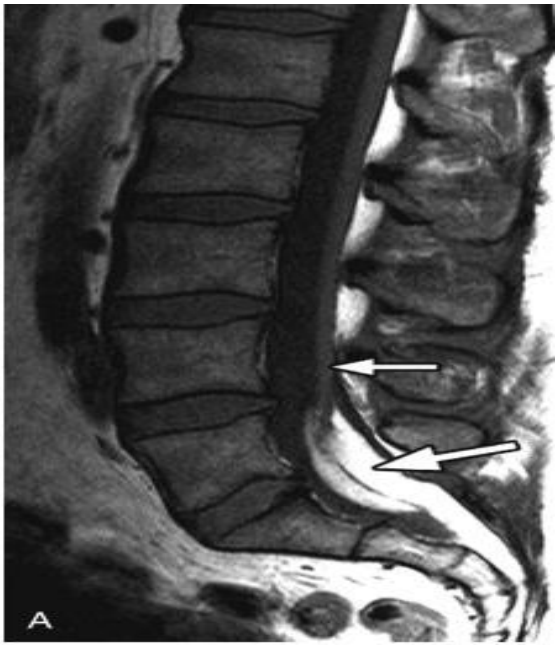

(A) Sagittal T1-weighted fat-saturated image

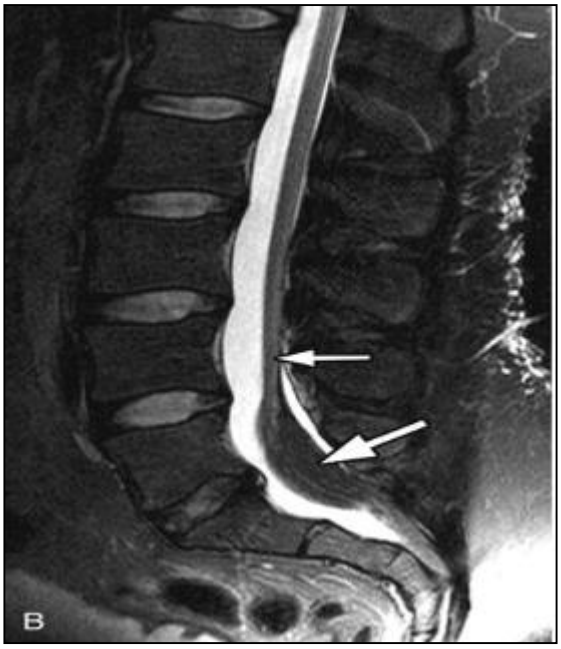

(B) T2-weighted

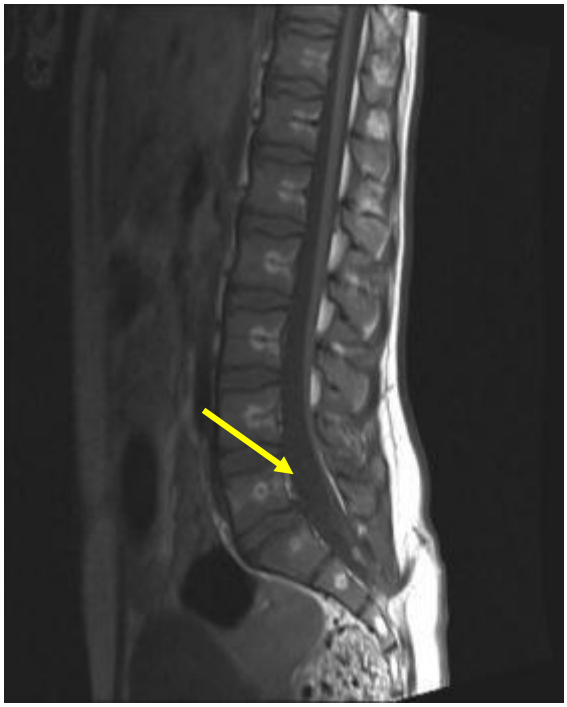

(C) Sagittal T1

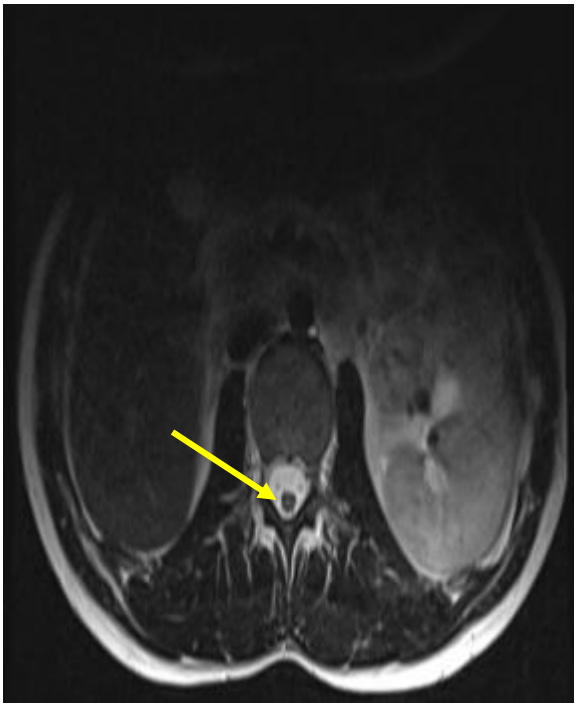

(D) Axial T2

DISCUSSION

Spinal cord dysfunction (SCDys), also known as injury to the spinal cord not caused by trauma, can have a wide range of diverse causes, including congenital, inflammatory, infectious, and tumour conditions [7]. In situations where CT is unable to accurately determine the aetiology of neurological impairments, MR imaging is often used as a problem-solving approach. The common clinical problems that need to be addressed when neurological signs are present, CT cannot properly explain them if spinal cord compression has occurred and whether extra-spinal lesions are evident [8]. Therefore, the purpose of this study was to evaluate the use of MRI in children with non-traumatic spinal injuries.

In this study, the most common type was intramedullary (48%) then extradural (36%) and intradural extramedullary (16%). The most common location was lumbar, cauda equina and lumbosacral (18%) than another location. The most common number of lesions was multiples (66%) then solitary (34%). This agrees with **Han *et al.*** [9] who showed that extradural tumors of the spine (including metastases) represent about 42.8%, intradural extramedullary tumors represent about 35.7% while intramedullary tumors represent about 21.5% of the spinal tumors. Also, according to **Izbudak *et al.*** [10]**,** the lumbar spine is also the most afflicted, followed by the thoracic, cervical, and sacral spines.

The present study showed that, most of patients were resident in rural (72%), 70% had pain, 40% had fever, and 48% had neurological deficits. In response to this concern, **Ülger *et al.*** [11] proposed that fever developing in SCI patients is a clinical condition known as "neurogenic fever", which is marked by a high rate of fatality. They discovered that 25 (48.1%) of 52 acute SCI patients were diagnosed with neurogenic fever during intensive care follow-up due to thermodysregulation, absence of response to treatment, and they also noted that fever was due to thermodysregulation secondary to SCI. Injury to the hypothalamus, the primary centre of the brain involved in thermoregulation, can result in thermodysregulation, particularly hyperthermia, even if the mechanism of fever onset after SCI is not entirely known [12].

This study showed that, paraspinal mass was 24 %, vertebral bone Involvement was 42%, Cord compression was 30% and Cord expansion was 0%. Extramedullary lesions accounted for 58.6% (range: 12-95%) of all lesions in **Musubire *et al.*** [13] comprehensive study. Compressive bone lesions accounted for 49.1% (range: 12-83%) of non-traumatic myelopathy patients in Africa, while non-bone compressive lesions accounted for 9.5% (range: 0-16%). While, 9.5% of patients had an unclear diagnosis (range: 0-45%), 31.9% of patients had non-compressive lesions (range: 5-97%). Undifferentiated transverse myelopathy accounted for 4.6% (range: 1-23%) of all diagnoses for non-compressive lesions [14, 16]. Transverse myelitis is often recognised on a plain radiograph by the lack of a compressive lesion and inflammatory CSF. The bulk of studies, however, were unable to identify the underlying causes of transverse myelitis.

Our results showed that, the most common MR diagnosis was myelomeningocele (18%) then meningitis (12%) followed by Focal Kyphus deformity, Guillain Barre Syndrome, Intramedullary abscess, astrocytoma (10%), osteoblastoma, lipoma, diastematomyelia (8%) and Tethered cord (6%). About 60–70% of patients with systemic cancer will have spinal metastases, according to a prior research by **Shah and Salzman** [17]**.** According to a research by **Müller-Jensen *et al.*** [18]**,** the three most common underlying diseases in their sample were compressive myelopathy brought on by spinal stenosis or disc herniation (19.4%), inflammatory spinal cord lesions (22.2%), and spinal metastases (33.3%). Spinal metastases comprised for 16.4–26.0% and inflammatory conditions 2.0–23.0% of NTSCI patients, respectively. Intriguingly, a research found that viral and inflammatory causes were most frequent among NTSCI patients who needed intensive care unit therapy [19]. Also, the imaging features of the case groups were retrospectively examined in a research by **Sun *et al.*** [20]**,** which also mentioned that meningomyelocele, meningocele, lipoma, sacrococcygeal bone hypoplasia, dermal sinus, tethered and tight FT and syringomyelia, etc. Meningomyelocele/lipo-myelomeningocele and meningocele/lipo-meningocele were more common in foetuses with tethered spinal cord (4/13) than in other children (6/20), respectively (46% vs. 30%). The most frequent concurrent abnormality in foetuses is meningomyelocele/lipo-myelomeningocele, which occurred in 10% (2/20) of infants with TCS.

Hyperintense T1WI was 46% in this investigation. T2WI with hyperintensity was 38%. On T1-weighted images, intradural neurilemmomas often exhibit signal intensities that are equal to or lower than those of the spinal cord and mild to pronounced hyperintensities on T2-weighted images. Cystic sections frequently correspond to focal regions of even higher hyperintensity on T2-weighted imaging, whereas hypointensity may signify haemorrhage, dense cellularity, or collagen deposition. Heterogeneity of the tumour does not always signify malignant transformation [21–22]. According to **Chung *et al.*** [23], neuroblastomas showed uniform enhancement on Gd-DTPA pictures, high signal intensity on T2-weighted images, and isointensity or intermediate signal intensity on T1-weighted images. On T1-weighted images, neurilemmomas had low signal intensity, but on T2-weighted images, they had high signal intensity.

Ependymomas may be isointense or hypointense to the spinal cord on T1WIs, but they are hyperintense on T2WIs, according to **Bloomer *et al.*** [24].

Areas of haemorrhage or cystic degeneration might be the cause of signal heterogeneity. **Nemoto and his Colleagues** [25] and **Fulbright *et al.*** [26] reported that by MRI, both ependymomas and astrocytomas were hypointense on T1W and hyperintense on T2W images with non-homogenous signals and hyper intense rim around the ependymomas in both sequences and defined this hyperintense rim associating ependymoma as pseudo capsule formed by repeated haemorrhages in the interface between the tumour and the normal cord.

Mehta's study [27] found that in type II Arnold-Chiari malformations, nerve roots with or without neural placode in thecal sac or outpouching were detected by 3D-MR Myelographic HASTE sequence with SE/TSE T1W sequence in all 24 cases having neural tissue malformation (48% of total patients), which suggested that this combination is extremely accurate to diagnose neural tissue (100% identification). Neural tissue detection rate with combination of other three pair of sequences viz. SE/TSE T1W and TSE T2W sequences, SE/TSE T1W and STIR sequences as well as SE/TSE T1W sequence with single shot myelographic sequences were 66.7%, 54.2% and 75%, which are significantly less as compared to combination of 3D-HASTE with SE/TSE T1W sequences having p-value of 0.002, <0.001 and 0.008 respectively. The presence of neural placode and nerves in dysraphism suggests a more complex deformity with a guarded prognosis.

According to a research by **Alshoabi *et al.*** [28]**,** the astrocytoma mostly displayed heterogeneous enhancement more in its margins in the contrast enhanced T1WIs. The septum pellucidum and splenium of the corpus callosum were both affected in the lesion, which seemed to be diffuse and infiltrative. On the coronal regions of the MRI, it also penetrated into both cerebral hemispheres, taking the shape of a butterfly. In this study, astrocytoma was found in 3 females in normal T1 and T2 and osteoblastoma was found in 3 females in hyperintense T1 and T2. Focal Kyphosis deformity was found in 5 females in normal T1and T2. Guillain Barre Syndrome was found in 5 females in normal T1and T2. Intramedullary abscess was found in 5 females in normal T1 and T2. Meningitis was found in 6 males in hyperintense T1 and T2. Meningocele was found in 4 males in hyperintense T1 and normal T2. Lipoma was found in 5 males in hyperintense T1 and T2. This supports the claim made by **Bloomer *et al.*** [24] that lipoma looks hyperintense on T1WIs, moderately low on T2WIs, and suppressed on fat-suppressed images. In order to address this issue, **Chamberlain and Tredway** [29] showed that ependymomas exhibit hyperintense signal on T2W images and hypo- or isointense signal to normal spinal cord on T1W pictures with heterogeneous contrast enhancement. These tumours may also exhibit syrinx, hemosiderin, and cystic alterations that are indicative of prior haemorrhage.

In this study, regarding post-contrast enhancement in MRI features, astrocytoma was found in 3 female. Guillain Barre Syndrome was found in 5 females. Meningitis was found in 6 males. In a study by **Alkan *et al.*** [30] found that due to the blood-nerve or blood-brain barrier, the spinal cord and nerve roots in the thecal sac often do not absorb much gadolinium during enhanced MR imaging. Therefore, a breach in the blood-nerve barrier is indicated by the noticeably increased nerve roots. Guillain-Barré Syndrome's inflammatory infiltration is suggested to be related to it [31]. Although it is a non-specific finding, enhancement of the spinal roots can be seen in neoplastic or other inflammatory processes, including meningeal carcinomatosis, sarcoidosis, lymphoma, AIDS-related cytomegalovirus polyradiculopathy, Lyme disease, postoperative arachnoiditis, and chronic inflammatory demyelinating polyneuropathy. These intradural-extramedullary diseases share Guillain-Barré Syndrome's characteristic protein elevation in the cerebrospinal fluid [32]. According to certain studies, contrast-enhanced MR imaging can be used to track a patient's response to treatment [33, 34]. Serial imaging may be helpful for tracking a patient's response to treatment [35].

CONCLUSIONS

In conclusion the current study showed that MRI is the best way in evaluation of non-traumatic spinal lesions in children. The most common MR diagnosis was meningitis (18%) then intramedullary abscess (12%), Focal Kyphus deformity, Guillain Barre Syndrome, osseous hemangioma, osteoblastoma and lipoma (10%).

REFERENCES

1. **Sastre-Garriga J, Pareto D, Battaglini M *et al.* (2020):** MAGNIMS consensus recommendations on the use of brain and spinal cord atrophy measures in clinical practice. Nature Reviews Neurology, 16 (3): 171-82.
2. **Santiago F, Ramos-Bossini A, Wáng Y *et al.* (2020):** The role of radiography in the study of spinal disorders. Quantitative Imaging in Medicine and Surgery, 10 (12): 2322-27.
3. **Kunam V, Velayudhan V, Chaudhry Z *et al.* (2018):** Incomplete cord syndromes: clinical and imaging review. Radiographics, 38 (4): 1201-22.
4. **Zou Z, Teng A, Huang L *et al.* (2021):** Pediatric spinal cord injury without radiographic abnormality: The Beijing experience. Spine, 46 (20): 1083-8.
5. **Kaufmann T, Smits M, Boxerman J *et al.* (2020):** Consensus recommendations for a standardized brain tumor imaging protocol for clinical trials in brain metastases. Neuro-oncology, 22 (6): 757-72.
6. **Kamble R (2021):** Magnetic resonance imaging brain sequences in pediatrics. Karnataka Pediatric Journal, 36 (1): 27-34.
7. **New P (2019):** A narrative review of pediatric nontraumatic spinal cord dysfunction. Topics in Spinal Cord Injury Rehabilitation, 25 (2): 112-20.

8. **Provenzale J (2007):** MR imaging of spinal trauma. Emergency Radiology, 13: 289-97.
9. **Han J, Kaufman B, El Yousef S *et al.* (1983):** NMR imaging of the spine. American Journal of Neuroradiology, 4 (6): 1151-9.
10. **Izbudak I, Tekes A, Baez J *et al.* (2008):** Imaging of spinal tumors. Imaging in Oncology. Springer Science+Business Media, LLC, Pp: 43-66. https://link.springer.com/chapter /10.1007/ 978-0-387-75587-8_2
11. **Ülger F, Pehlivanlar Küçük M, Öztürk Ç *et al.* (2019):** Non-infectious fever after acute spinal cord injury in the intensive care unit. The Journal of Spinal Cord Medicine, 42 (3): 310-7.
12. **McKinley W, McNamee S, Meade M *et al.* (2006):** Incidence, etiology, and risk factors for fever following acute spinal cord injury. The Journal of Spinal Cord Medicine, 29 (5): 501-6.
13. **Musubire A, Meya D, Bohjanen P *et al.* (2017):** A systematic review of non-traumatic spinal cord injuries in sub-Saharan Africa and a proposed diagnostic algorithm for resource-limited settings. Frontiers in Neurology, 8: 618-22.
14. **Parry O, Bhebhe E, Levy L (1999):** Non-traumatic paraplegia [correction of paraplegis] in a Zimbabwean population--a retrospective survey. The Central African Journal of Medicine, 45 (5): 114-9.
15. **Nyame P (1994):** An aetiological survey of paraplegia in Accra. East African Medical Journal, 71 (8): 527-30.
16. **Looti A, Kengne A, de Paul Djientcheu V *et al.* (2010):** Patterns of non-traumatic myelopathies in Yaounde (Cameroon): a hospital-based study. Journal of Neurology Neurosurgery & Psychiatry, 81 (7): 768-70.
17. **Shah L, Salzman K (2011):** Imaging of spinal metastatic disease. International Journal of Surgical Oncology, 11: 769753. doi: 10.1155/2011/769753.
18. **Müller-Jensen L, Ploner C, Kroneberg D *et al.* (2021):** Clinical presentation and causes of non-traumatic spinal cord injury: An observational study in emergency patients. Frontiers in Neurology, 12: 701927. doi: 10.3389/fneur.2021.701927
19. **Grassner L, Marschallinger J, Dünser M *et al.* (2016):** Nontraumatic spinal cord injury at the neurological intensive care unit: spectrum, causes of admission and predictors of mortality. Therapeutic Advances in Neurological Disorders, 9 (2): 85-94.
20. **Sun Y, Ning G, Li X *et al.* (2022):** MRI characteristics of the fetal tethered spinal cord: a comparative study. International Journal of Neuroscience, 132 (10): 975-84.
21. **Parizel P, Balériaux D, Rodesch G *et al.* (1989):** Gd-DTPA-enhanced MR imaging of spinal tumors. American Journal of Neuroradiology, 10 (2): 249-58.
22. **Friedman D, Tartaglino L, Flanders A (1992):** Intradural schwannomas of the spine: MR findings with emphasis on contrast-enhancement characteristics. American Journal of Roentgenology, 158 (6): 1347-50.
23. **Chung J, Lee J, Kim H *et al.* (2008):** Characterization of magnetic resonance images for spinal cord tumors. Asian Spine Journal, 2 (1): 15-21.
24. **Bloomer C, Ackerman A and Bhatia R (2006):** Imaging for spine tumors and new applications. Topics in Magnetic Resonance Imaging, 17 (2): 69-87.
25. **Nemoto Y, Inoue Y, Tashiro T *et al.* (1992):** Intramedullary spinal cord tumors: significance of associated hemorrhage at MR imaging. Radiology, 182 (3): 793-6.
26. **Fulbright R, Ross J, Sze G (1993):** Application of contrast agents in MR imaging of the spine. Journal of Magnetic Resonance Imaging, 3 (1): 219-32.
27. **Mehta D (2017):** Magnetic resonance imaging in paediatric spinal dysraphism with comparative usefulness of various magnetic resonance sequences. Journal of Clinical and Diagnostic Research, 11 (8): 17-22.
28. **Alshoabi S, Alareqi A, Omer A *et al.* (2021):** Diffuse astrocytoma and the diagnostic dilemma of an unusual phenotype: A case report. Radiology Case Reports, 16 (2): 319-26.
29. **Chamberlain M, Tredway T (2011):** Adult primary intradural spinal cord tumors: a review. Current Neurology and Neuroscience Reports, 11: 320-8.
30. **Alkan O, Yildirim T, Tokmak N *et al.* (2009):** Spinal MRI Findings of Guillain-BarrÃ© Syndrome. Journal of Radiology Case Reports, 3 (3): 25-8.
31. **JAIN, Esha, et al. Facial diplegia:** a rare, atypical variant of Guillain-Barré syndrome and Ad26. COV2. S vaccine. *Cureus*, 2021, 13.7.
32. **Baran G, Sowell M, Sharp G *et al.* (1993):** MR findings in a child with Guillain-Barré syndrome. American Journal of Roentgenology, 161 (1): 161-3.
33. **Coşkun A, Kumandaş S, Paç A *et al.* (2003):** Childhood Guillain-Barré syndrome: MR imaging in diagnosis and follow-up. Acta Radiologica, 44 (2): 230-5.
34. **Iwata F, Utsumi Y (1997):** MR imaging in Guillain-Barré syndrome. Pediatric Radiology, 27: 36-8.
35. **Byun W, Park W, Park B *et al.* (1998):** Guillain-Barré syndrome: MR imaging findings of the spine in eight patients. Radiology, 208 (1): 137–41.